

Supporting Information

Elucidating sequence and solvent specific design targets to protect and stabilize enzymes for biocatalysis in ionic liquids

K. G. Sprenger¹, J. G. Plaks², J. L. Kaar², and J. Pfaendtner^{1,*}

¹Department of Chemical Engineering, University of Washington, Seattle,
Washington 98105

²Department of Chemical and Biological Engineering, University of Colorado,
Boulder, Colorado 80309

*Corresponding Author: E-mail: jpfaendt@uw.edu

Table S1. Characterization of cation binding sites on the surface of WT-lipA as determined through a combined experimental and computational approach (see Computational Methods, main text).

Binding Site	Residue Numbers*	Amino Acids	Site Color
1	27, 33	VAL, ARG	Blue
2	89, 90	ASN, LEU	Red
3	152	HIS	Purple
4	157, 161	ILE, TYR	Dark Pink
5	44, 45	LYS, THR	Yellow
6	12, 13, 108	ILE, GLY, LEU	Cyan
7	107, 142, 144	ARG, ARG, ASP	Green
8	42,49	TRP, TYR	Light Pink
9	119	PRO	Violet
10	17	PHE	Black
11	37	TYR	Orange
12	134,135, 137,139	MET, ILE, MET, TYR	Gray

*Consistent with numbering in PDB code 5CRI

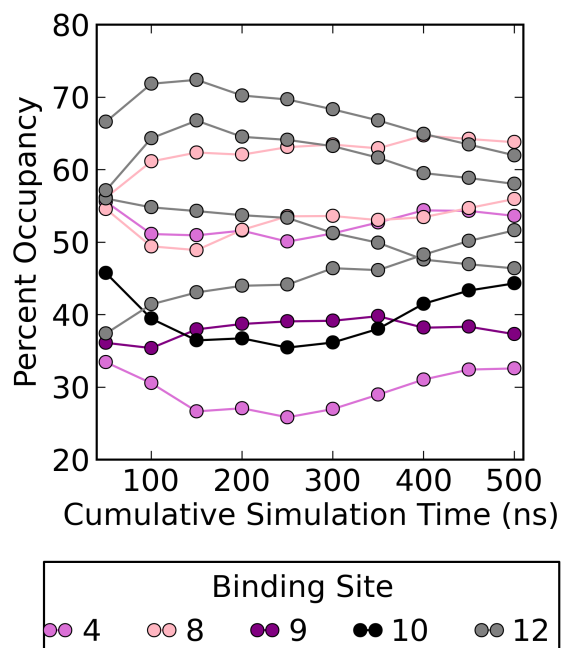


Figure S1. Percent occupancy of WT-lipA residues by IL cations, calculated over increasing periods of simulation time, for the residues in the top five cation-binding sites identified from the experimental crystal structures.

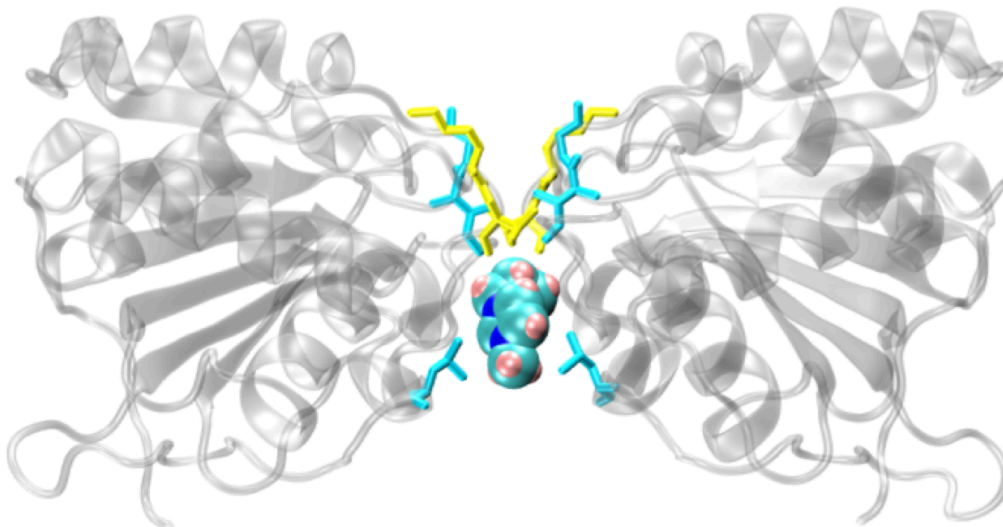


Figure S2. Snapshot of an IL cation stabilized between two proteins in the crystal structure of lipA in 20% aqueous IL solution (PDB code 5CT6). Residues in binding sites 5 (yellow) and 6 (cyan) are shown in licorice representation. The IL cation is shown in van der Waals representation with carbon, nitrogen, and hydrogen atoms shown in cyan, blue, and pink, respectively.

Additional Metrics for Binding Site Clarification

The residence time distribution ($rtd(\Delta\tau_k)$) for an IL cation ([BMIM]) around a given residue in lipase was calculated via the following correlation function:

$$rtd(\tau_k) = \sum_{j=1}^{N_{tmax}-k} \sum_{i=1}^{N_{[BMIM]}} v_i(t_j)v_i(t_j + \tau_k), \quad (1)$$

$$k = 0, 1, \dots, (N_{tmax} - 1),$$

where τ_k is the k^{th} time interval ($\tau_k = k\Delta\tau$ and $\Delta\tau = 20$ ps). In Equation 1, $v_i(t)$ acquires a value of 0 or 1 depending if any atom within the i^{th} cation molecule is outside or inside, respectively, a 4\AA radius shell surrounding the enzyme at time t . Figure S3 shows the IL cation residence time around each residue in WT-lipA for the different IL concentrations. We note that the trends of Figure S3 are not dependent upon the size of the time window ($\Delta\tau$) we chose to perform the

calculations; results are similar over the range in window size from 20-200 ps (data not shown), thus ensuring that the re-migration of a cation molecule into the hydration shell after vacating it for some time does not influence the results.

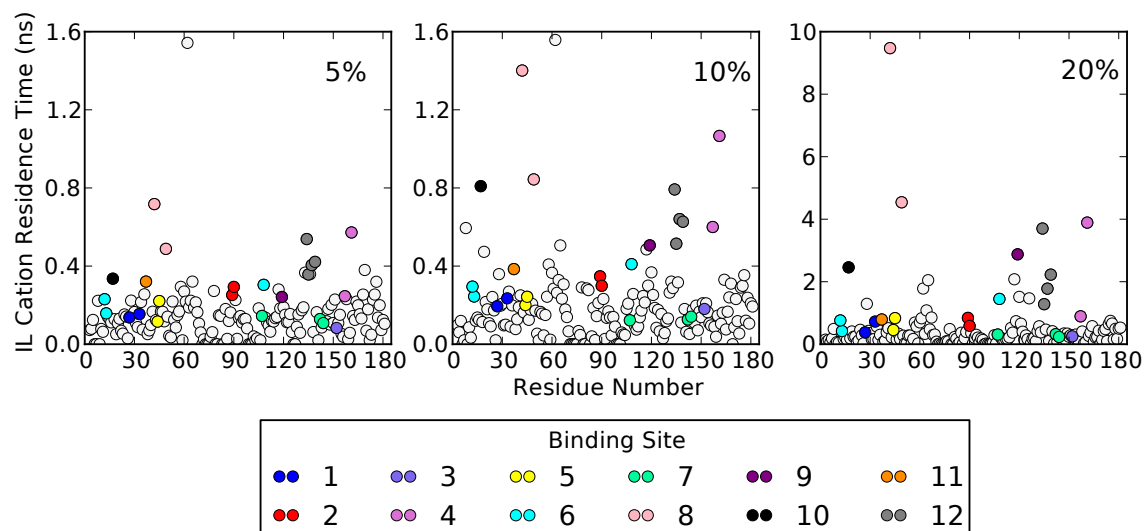


Figure S3. Residence time of IL cation binding to residues in WT-lipA as a function of IL concentration in water. Colored circles represent experimentally identified binding sites, and uncolored circles represent all other protein residues.

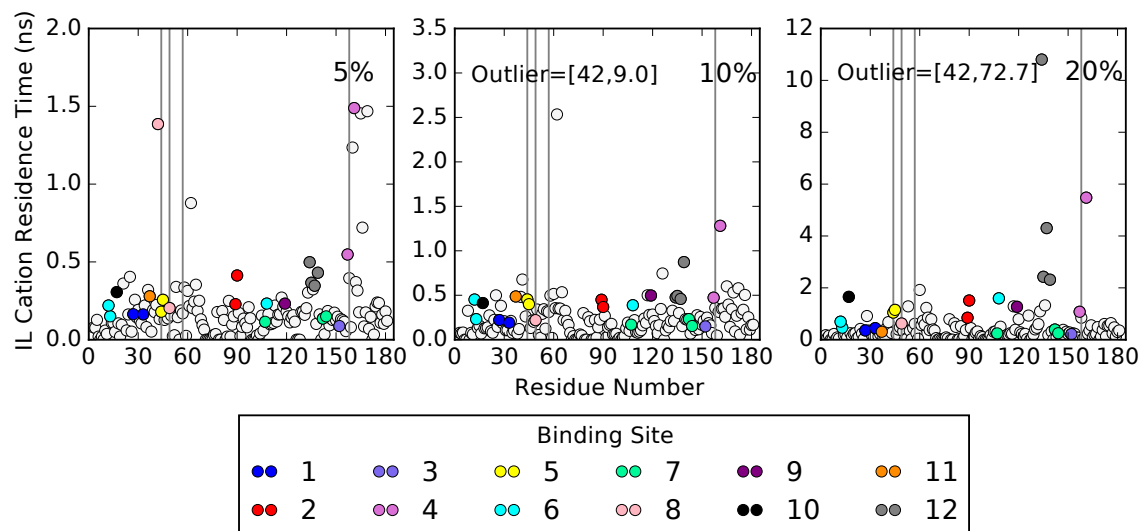


Figure S4. Residence time of IL cation binding to residues in QM-lipA as a function of IL concentration in water. Colored circles represent experimentally identified binding sites, and uncolored circles represent all other protein residues. Vertical gray lines correspond to residues mutated in mutagenesis experiments.

In general, the results for residence time are less consistent across the different IL concentrations than the occupancy results of Figure 2 (main text). Our hypothesis is that the significantly higher residence times for the 20% IL solution likely reflect a change from a dilute salt solution (5/10% IL) where water can effectively shield the electrostatic effects of ILs, to a concentrated salt solution where electrostatics dominate and lead to significant reductions in diffusion of IL ions to and from the enzyme surface. Another factor that could contribute is the possibility of cations swapping places near a given lipase residue from one time to the next, which our script would not be able to distinguish and this would be much more likely to occur in the concentrated 20% IL solution.

Figure S3 provides some new information in regards to residue V62, which shows a high cation residence time at all IL concentrations, indeed the highest residence time of all residues in lipase for the 5 and 10% IL solutions. This is especially interesting because the occupancy values in Figure 2 (main text), while of significance, do not indicate V62 to be nearly as important as Figure S3 does. The contrast between these two metrics can be understood by considering the stability and location of V62 on the enzyme's surface: its exposure to solvent is limited by its location on the underside of a helix (Figure S4), hindering cation diffusion to the site, however this same location on a structured region of the enzyme (as opposed to a flexible loop region), combined with a short sidechain length, leads to strong interactions with cations once they are bound. The above analysis provides a case

for using multiple metrics to gain a complete picture of IL binding to the surface of an enzyme.

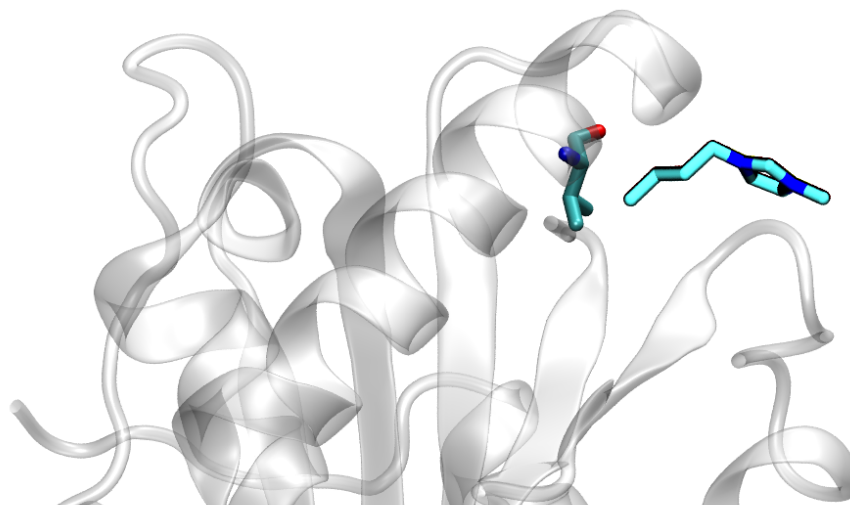


Figure S5. Simulation snapshot from the 5% IL solution simulation highlighting the location of residue 62 (valine) on the surface of lipase (in gray) and its interaction with an IL cation. Hydrogen atoms not pictured.

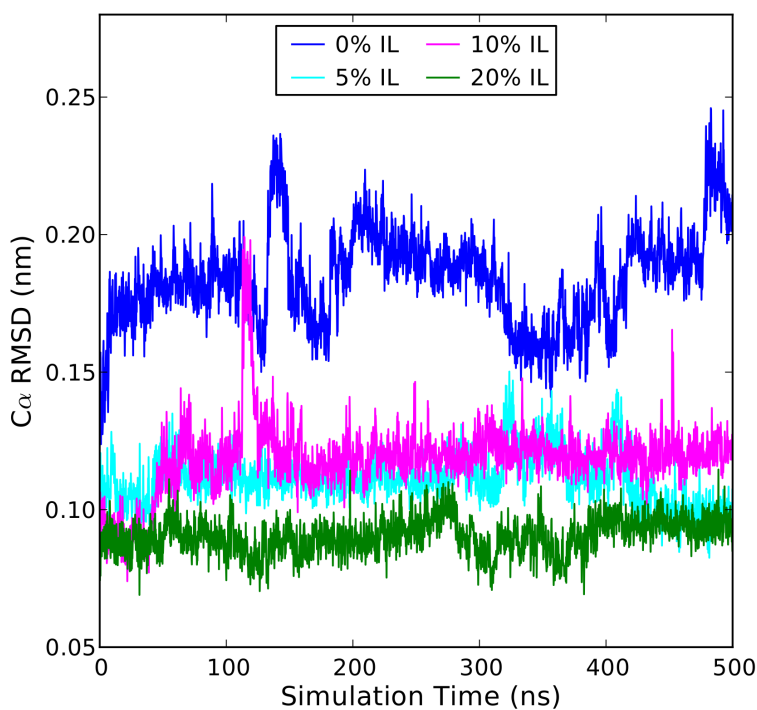


Figure S6. Time series of the root-mean-squared deviation (RMSD) of distances between C α atoms in WT-lipA for each of the different IL concentrations studied. Data was collected from the trajectory every 20 ps and plotted every 10th point.

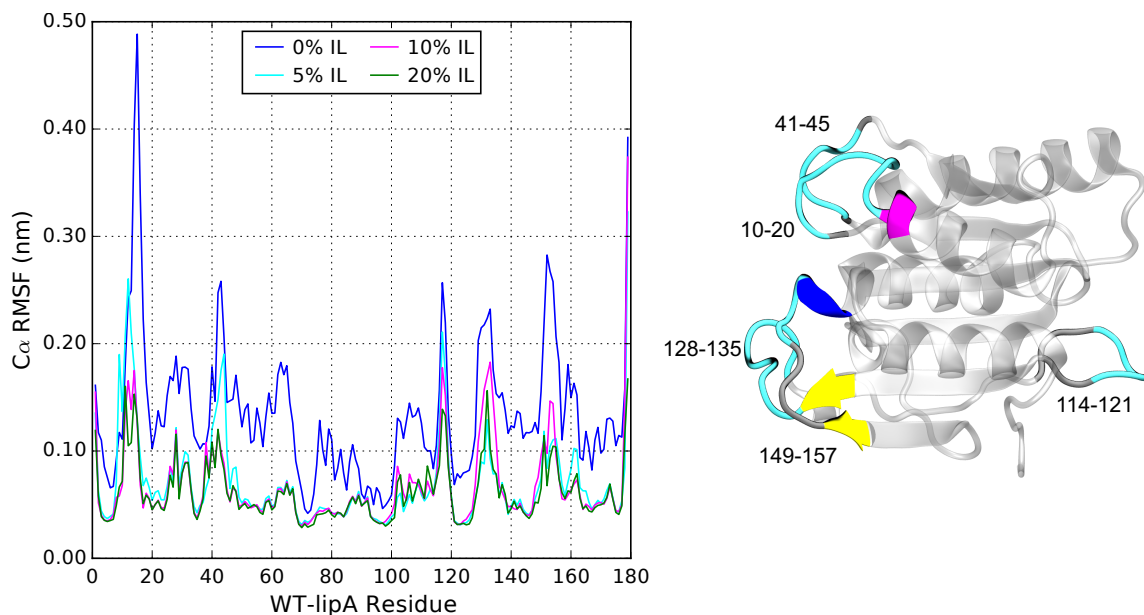


Figure S7. (left) Time series of the root-mean-squared fluctuation (RMSF) of C_{α} atoms (sequence) in WT-lipA for each of the different IL concentrations studied. (right) crystal structure of WT-lipA, highlighting regions of high RMSF values. Number ranges next to highlighted areas indicate the corresponding sequence range. Magenta and blue coloring indicate α - and 3_{10} -helices, respectively, and yellow, cyan, and dark gray coloring indicate β -sheets, turns, and random coils, respectively.

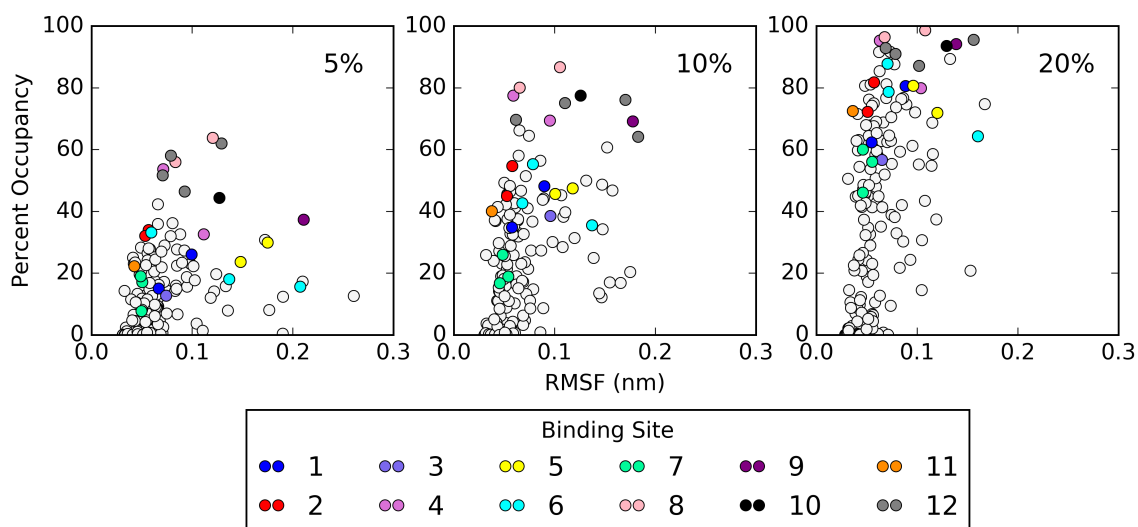


Figure S8. RMSF vs. percent occupancy of residues in WT-lipA by IL cations as a function of IL concentration in water. Colored circles represent experimentally identified binding sites, and uncolored circles represent all other protein residues.

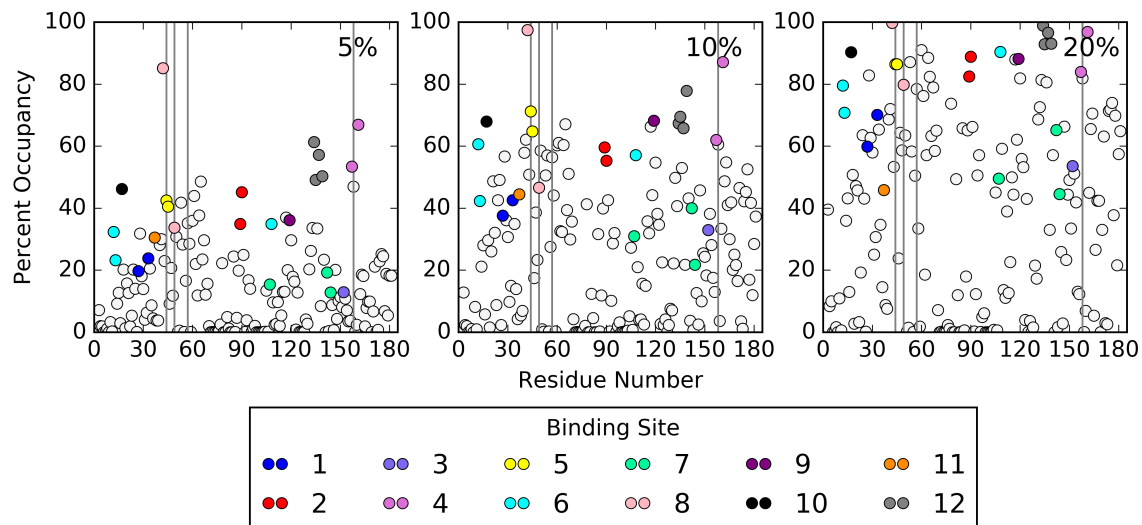


Figure S9. Percent occupancy of residues in QM-lipA by IL cations as a function of IL concentration in water. Colored circles represent experimentally identified binding sites, and uncolored circles represent all other protein residues. Vertical gray lines correspond to residues mutated in mutagenesis experiments.

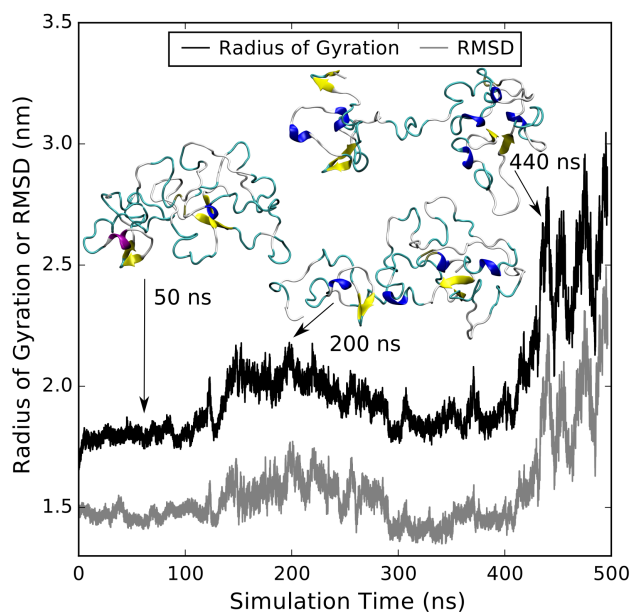


Figure S10. Radius of gyration and RMSD (relative to the crystal structure) of denatured WT-lipA versus time with corresponding simulation snapshots (insets).